J. Chem. Sci. Vol. 128, No. 2, February 2016, pp. 227–234. © Indian Academy of Sciences.
DOI 10.1007/s12039-015-1018-4

Ammoxidation of 2-methyl pyrazine to 2-cyano pyrazine on $MoO_3/FePO_4$ catalysts

NAGARAJU PASUPULETY[a,*], HAFEDH DRISS[b], YAHIA ABOBAKOR ALHAMED[a,b], ABDULRAHIM AHMED ALZAHRANI[a,b], MUHAMMAD A DAOUS[a,b], LACHEZAR PETROV[a], N LINGAIAH[c] and P S SAI PRASAD[c]

[a]SABIC Chair of Catalysis, King Abdulaziz University, P.O. Box 80204, Jeddah 21589, Saudi Arabia
[b]Chemical and Materials Engineering Department, Faculty of Engineering, King Abdulaziz University, P.O. Box 80204, Jeddah 21589, Saudi Arabia
[c]Inorganic & Physical Chemistry Division, Indian Institute of Chemical Technology, Hyderabad 500 007, India
e-mail: pasupulety@gmail.com

MS received 27 September 2015; revised 3 November 2015; accepted 20 November 2015

Abstract. The objective of this work is to understand the influence of small amount of Mo=O (1, 3 and 5 wt.% MoO_3) impregnated on $FePO_4$ and its resultant effect on the acidity was studied for the ammoxidation of 2-methyl pyrazine (2-MP) to 2-cyano pyrazine (2-CP) in the temperature range of 380–420°C. The Mo/FeP catalyst characteristics were evaluated by XRD, HAADF-EDS, TPR and NH_3-TPD techniques. Primarily, quartz-type XRD phase was observed for the iron phosphate (FeP). The Mo/FeP exhibits MoO_3 and quartz-type iron phosphate phase. The interface between Mo particles (20 nm) and FeP was clearly established by HR-TEM in 3Mo/FeP. Furthermore, the average atomic composition revealed by HAADF/EDS for 3Mo/FeP as Fe 30.0%, P 40.0% and Mo 1.6% with Fe/Mo surface XPS ratio 6. The greater 2-CP yield of 68.0% on 3Mo/FeP was attributed to enhanced, moderate acid sites coming from MoO_3 and cooperation between Mo and FeP at the interface in terms of oxygen and electron transfer to the reactant (2-MP).

Keywords. Iron phosphate; molybdenum; ammoxidation; 2-methyl pyrazine.

1. Introduction

Ammoxidation catalysis involves the catalytic oxidation of alkyl moiety of an organic molecule in the presence of ammonia that incorporates a nitrile functionality into the molecule. Virtually, the molecules that can undergo selective catalytic oxidation to an aldehyde can also undergo selective ammoxidation to produce the corresponding nitrile. For example, 2-methyl pyrazine (2-MP) can be oxidized to pyrazine 2-carbaldehyde/acid using an iron phosphate catalyst. In the presence of ammonia, over the same catalyst, pyrazine 2-carbaldehyde/acid is ammoxidized to the corresponding nitrile molecule, 2-cyano pyrazine (2-CP) (scheme 1). Nonselective reactions that produce the complete oxidation products such as CO, CO_2 and H_2O, are thermodynamically more favorable than the selective ammoxidation reactions.[1] Selective nitrile generation via ammoxidation in useful yields, thus, need the use of a suitable catalyst to enhance its rate over nonselective complete oxidation reactions. In general, (amm)oxidation step requires transfer of surface/lattice oxygen and transfer of electrons between the reactant molecule and the surface active site. Each of the steps presents the opportunity for a less than optimum reaction that forms waste products, like pyrazine, CO and CO_2. The optimal active site composition near the catalyst surface is necessary for nitrile incorporation to produce 2-CP. In this context, our group was working on selective and active catalyst developments such as iron phosphate for 2-MP ammoxidation to 2-CP. In our previous studies 2-CP yield of 45.0% was reported for iron phosphate with P/Fe atomic ratio 1.2.[2,3] Furthermore, enhanced 2-CP yield (50.0%) was obtained by introducing a small amount of vanadium in to this catalyst.[4] MoO_3 supported on TiO_2, ZrO_2 and ZrO_2-Al_2O_3 was employed as an ammoxidation catalyst.[5,6] However, high temperature activity and complete oxidation was the drawback of these catalysts. Ai *et al.*[7,8] studied the catalytic activity of iron phosphates doped with a small amount of molybdenum and palladium in the oxidative dehydrogenation of lactic acid to pyruvic acid. It is well known that Mo(V) to Mo(VI) oxidation-reduction is very rapid[8] and there is an existing opportunity to construct an optimal catalyst composition for 2-MP to 2-CP transformation by adding a certain

*For correspondence

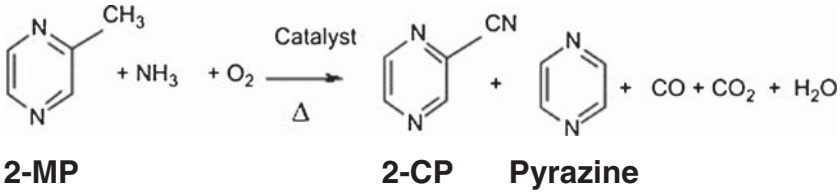

Scheme 1. Generalized 2-MP ammoxidation pathway.

amount of Mo=O (MoO_3) functionality to FeP moiety. To the best of our knowledge, it is the first report to study the Mo/FeP catalytic activity for the 2-MP ammoxidation reaction. Therefore, the significance of this work is to understand the catalytic aspects of Mo/FeP in the production of 2-CP. Furthermore, the Fe and Mo average composition was examined by HAADF/EDS technique. The acidity of Mo/FeP was estimated by NH_3-TPD studies and correlated with 2-CP selectivity.

2. Experimental

2.1 *Reagents*

$Fe(NO_3)_3.9H_2O$ ($\geq$ 99.0%), H_3PO_4 ($\geq$ 85.0%), 2-MP ($\geq$ 99.0%) and $(NH_4)_6Mo_7O_{24}{\cdot}4H_2O$ ($\geq$ 99.9%) were purchased from Sigma-Aldrich chemical suppliers and used without any further purification.

2.2 *$FePO_4$ synthesis*

In a typical procedure for P/Fe = 1.2,[9] 65.0 g of iron(III) nitrate and 23.0 g of ammonium dihydrogen phosphate were dissolved in 250 cm^3 deionized water. The resultant solution was aged for 2 h and the excess water was removed on a preheated hot plate (120°C) under continuous stirring. The obtained solid masses crushed into powder and dried in a preheated oven at 120°C for 12 h under static air.

2.3 *$MoO_3/FePO_4$ synthesis*

Addition of 1, 3 and 5 wt.% equivalent molybdenum to the above prepared iron phosphate was done by using ammonium heptamolybdate precursor. For example, to get approximately 3 wt.% molybdenum, 0.55 g of ammonium heptamolybdate dissolved in 50 cm^3 deionized water was added to 9.45 g of FeP and aged for 2 h. The excess water was evaporated on a preheated hot plate (120°C) under continuous stirring. The subsequent paste was dried in a preheated oven (120°C) for 12 h under static air.

Finally, all the catalyst samples were calcined at 550°C for 4 h under static air. The synthesized bulk iron phosphate is denoted as FeP and the molybdenum supported iron phosphate catalysts are denoted as 1Mo/FeP, 3Mo/FeP and 5Mo/FeP. Here the prefix 1, 3 and 5 refers to the Mo loading wt.% on the iron phosphate.

2.4 *Characterization of fresh catalysts*

BET surface area of helium pretreated (200°C, 2 h) sample was estimated on a Micromeritics Auto Chem-2910 instrument at liquid nitrogen temperature. XRD pattern of calcined sample was obtained on a Rigaku Miniflex diffractometer, using Cu K_α radiation (λ = 1.54 Å). The measurement was recorded in the 2θ range of 2 to 80° with step size of 0.02°. MoO_3 crystallite size (D) at $2\theta = 27.2°$ was calculated by Scherrer equation.

$$D = \frac{0.9\lambda}{\beta \cos\theta}$$

where, λ is the X-ray wavelength 1.54 Å, β is full-width at half-maximum (FWHM) of the X-ray peak and θ is Bragg diffraction angle.

High resolution transmission electron microscopy (HR-TEM), scanning transmission electron microscopy (STEM), high angle angular dark field (HAADF) and energy dispersive X-ray (EDS) analysis results of the calcined samples were collected on Tecnai 200 kV D1234 SuperTwin microscope with camera length of 97 cm.

Temperature programmed reduction (TPR) of the calcined samples were carried out under 10% H_2-Ar atmosphere at 30 cm^3/min flow rate. About 0.1 g of sample was pretreated under helium atmosphere (20 cm^3/min) at 200°C for 2 h prior to the TPR run. The hydrogen consumption was monitored by using a thermal conductivity detector (TCD) in the temperature range of 30–1030° C at a ramp rate of 10°C/min.

The acidity of the calcined sample was measured by Temperature programmed desorption (TPD) of ammonia. In a typical experiment, about 0.1 g of catalyst was pretreated under helium atmosphere (20 cm^3/min) at 200°C for 2 h. Subsequently, the catalyst was brought to room temperature and saturated with probe gas (10%

NH_3-He). Desorption of probe gas was performed after 1 h of helium flushing over a temperature range of 30–800°C at a ramping rate of 10°C/ min. The desorbed gas was monitored by using a TCD detector.

XPS measurements of the calcined sample was done on a Kratos Axis 165 apparatus equipped with a dual anode (Mg and Al) using the MgK_α source. The carbon 1s binding energy of 284.6 eV was used as a reference for determining the sample binding energies.

2.5 *Catalytic reaction*

Vapor phase ammoxidation of 2-MP was carried out in a fixed-bed flow reactor in in the temperature range of 380 to 420°C under atmospheric pressure. In a typical experiment, about 3.0 g of the catalyst was loaded in the reactor between two quartz plugs. The reactant feed with a molar ratio of 2-MP: water: ammonia: air = 1: 13: 17: 38 was fed into the preheated portion of the reactor. The aqueous mixture of 2-MP was metered using a microprocessor based feed pump (B. Braun, Germany), at a flow rate of 2 cm^3/h. After 0.5 h at each reaction temperature, the liquid product was collected for 10 min and it was analyzed using PerkinElmer gas chromatograph equipped with SE-30 packed column (2 m long, 3 mm dia) and FID. The gas products were collected in a gas trap and analyzed using Restek Plot Q column connected to the TCD. The calibrated results were reproducible within ±1 % error. The CO, CO_2 and unknown product formation were found to be in the range of 1-3% with maximum selectivity of 1-7%. Pyrazine was the major byproduct in the 2-MP ammoxidation reaction (scheme 1).

The conversion of 2-MP, selectivity and yield of the detected products was calculated based on the following equations (1)–(3):

$$\%X_{2\text{-MP}} = \frac{(\text{Moles of 2-MP, } \mathbf{in} - \text{Moles of 2-M, } \mathbf{out})}{\text{Moles of 2-MP, } \mathbf{in}} \times 100 \quad (1)$$

$$\%S_i = \frac{\text{Moles of product } i \ \mathbf{out}}{(\text{Moles of 2-MP, } \mathbf{in} - \text{Moles of 2-MP, } \mathbf{out})} \times 100 \quad (2)$$

$$\%Y_i = \frac{\text{Moles of product } i \ \mathbf{out}}{\text{Moles of 2-MP, } \mathbf{in}} \times 100 \quad (3)$$

3. Results and Discussion

3.1 *XRD*

XRD pattern for FeP and Mo/FeP are presented in figure 1. FeP displays main reflection at $2\theta = 20.2$ and 25.8° which corresponds to quartz (Q) type phase.[10] In all the three Mo/FeP samples, XRD reflections were pronounced at similar 2θ values due to FeP quartz phase. On the other hand, MoO_3 exhibits main reflections at $2\theta = 23.8$, 25.5 and 27.2° which correspond to orthorhombic phase [JCPDS 35-609]. However, upon Mo addition to FeP, new reflections appeared at $2\theta = 23.8$ and 27.2°. Weak reflection was observed at $2\theta = 27.2°$ for 1Mo and 3Mo/FeP whereas, 5Mo/FeP showed intense XRD reflections at $2\theta = 23.8$ and 27.2° corresponds to the orthorhombic MoO_3 phase. The MoO_3 crystallite size for Mo/FeP catalysts were estimated by Scherrer equation and the obtained crystallite size is listed in table 1. The MoO_3 crystallite size increased from 1 (12 nm) to 5 wt.% (45 nm) of Mo loading on FeP. The results suggest the presence of small sized/dispersed MoO_3 crystallite up to 3 wt.% of Mo loading and after this loading existence of aggregated Mo crystallite on FeP is indicated. In our previous report for vanadium doped iron phosphates, the excess phosphorous on FeP was chemically interacted with vanadium to produce $(VO)_2P_2O_7$.[4] Transformation of molybdenum phosphorous salts in the pretreatment temperature range of 500–600°C to molybdenum oxypyrophosphate ($(MoO_2)_2P_2O_7$) was reported in the literature with *in situ* X-ray reflection at $2\theta = 23.0°$.[11] In the present study, Mo-P-O related phases were not

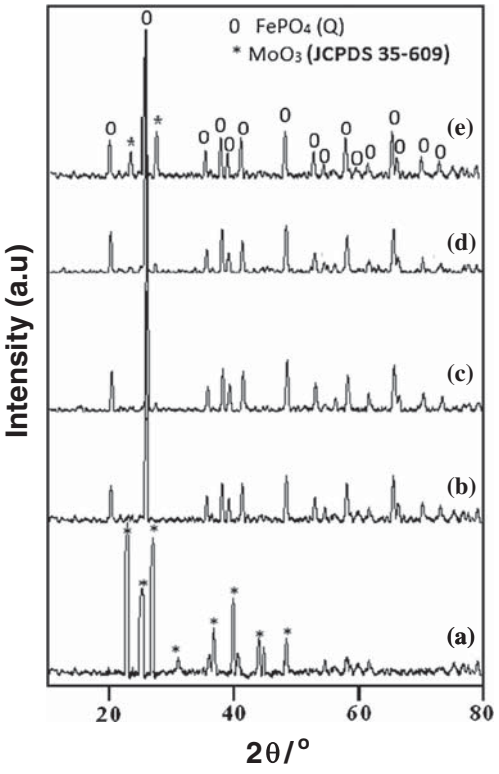

Figure 1. XRD patterns for (a) MoO_3, (b) FeP, (c) 1Mo/FeP, (d) 3Mo/FeP and (e) 5Mo/FeP.

detected by XRD. The BET surface area results for FeP, MoO_3 and Mo/FeP samples are presented in table 1. The estimated BET surface area for MoO_3 was found to be 40.0 m^2/g. FeP exhibited the BET surface area of 3.8 m^2/g and the Mo/FeP sample showed the BET surface area in the range of 3.5-2.2 m^2/g.

3.2 *HAADF/EDS*

HAADF images for Mo/FeP are presented in figure 2. The FeP (figure 2a) displayed a nodular type particles whereas, Mo/FeP displayed spherical bright spots on nodular particles. The nodular particles are characteristic feature of Fe-P-O frame-work. The EDS analysis revealed the bright spherical particles are made up of Mo and oxygen (figure 2e). It is clear from figure 2b that, at 3 wt.% Mo loading, the MoO_3 particles are dispersed on the surface of the FeP 15-25 nm size range. On the other hand, at higher loadings (5 wt.%) the MoO_3 particles are aggregated with 40 nm size. Figure 2c, shows the HR-TEM image for possible MoO_3/FeP interface. Mehri *et al.*[12] studied V_2O_5/TiO_2 catalysts in the ammoxidation of toluene and the authors reported the benzonitrile

Table 1. BET surface area, HAADF/EDS composition, H_2-TPR and NH_3-TPD results for MoO_3, FeP and Mo/FeP catalysts.

Catalyst	BET m^2/g	MoO_3 (nm)[a]	HAADF/EDS (at.%) Fe	P	Mo	HAADF Mo (nm)	H_2-TPR (μmol/g)	NH_3TPD(μmol/g) medium	strong	XPS Fe/Mo ratio
MoO_3	40.0	–	–	–	–	–	6.30	450.0	50.0	–
FeP	3.8	–	34.0	44.0	–	–	8.12	260.0	723.0	–
1Mo/FeP	3.5	12.0	32.0	43.0	0.60	10.0	8.25	300.0	630.0	10.0
3Mo/FeP	3.0	22.0	30.0	40.0	1.6	20.0	8.38	360.0	541.0	6.0
5Mo/FeP	2.2	45.0	25.0	36.0	2.4	40.0	8.50	428.0	432.0	2.5

[a]Calculated using Scherrer equation at XRD signal $2\theta = 27.2°$

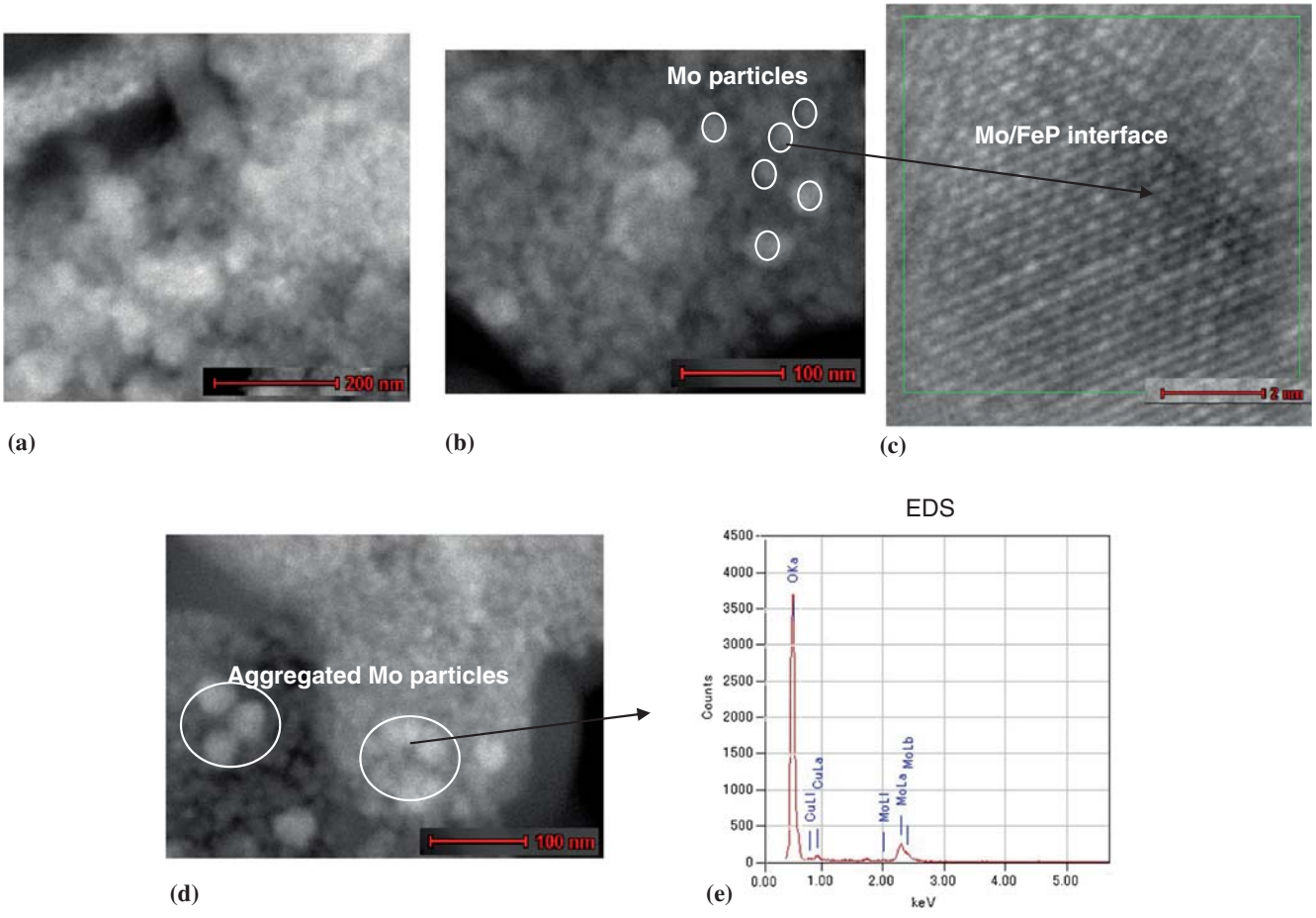

Figure 2. (a) HAADF image of FeP (b) HAADF image of 3Mo/FeP (c) HR-TEM image of 3Mo/FeP interface (d) HAADF image of 5Mo/FeP (e) EDS of 5Mo/FeP catalyst.

formation at V_2O_5/TiO_2 interface. In present study, we believe that the transformation of electrons/oxygen between the Mo/FeP interface and the 2-MP generated 2-CP and pyrazine. The EDS analysis data for Fe, P and Mo elements are presented in table 1. The results showed a slight decrease in the surface P and Fe content in Mo/FeP. It might be associated with the shielding of FeP surface to some extent by MoO_3.

3.3 *TPR*

The reduction behavior of calcined FeP, MoO_3 and Mo/FeP is displayed in figure 3. The corresponding total hydrogen consumption quantities are listed in table 1. Three stage reduction behavior was observed for FeP (figure 3b). The corresponding three signals centered at 560, 670 and 770°C. The first stage reduction (560°C) behavior associated with $FePO_4$ to $Fe_3(P_2O_7)_2$, second stage (670°C) associated with $Fe_3(P_2O_7)_2$ to $Fe_2P_2O_7$ and the final stage reduction behavior (770°C) was due to $Fe_2p_2O_7$ to Fe^0.[10] The MoO_3 mainly showed two stage reduction behavior (figure 3a) with signal maxima at 810 and 990°C. Thomas *et al.*[13] reported similar two stage reduction behavior for Mo^{6+} to Mo^{4+} and Mo^{4+} to Mo^0. Apart from this, a small shoulder appeared at 765°C might be associated with reduction of dispersed MoO_3 into Mo_4O_{11}.[13] After the addition of molybdenum to FeP, similar reduction signals pronounced due to FeP. However, the reduction steps due to $FePO_4$ to $Fe_3(P_2O_7)_2$ and $Fe_3(P_2O_7)_2$ to $Fe_2P_2O_7$ shifted to higher temperature form 1Mo to 3Mo to 5Mo/FeP (figure 3, dotted lines). Furthermore, the hydrogen consumption seems to be higher for $Fe_2P_2O_7$ to Fe^0 step (770°C) in all the three Mo/FeP catalysts. On the other hand, $Fe_3(P_2O_7)_2$ to $Fe_2P_2O_7$ (670°C) was the major reduction step for FeP. Rensen *et al.*[14] reported TPR studies on $FePO_4$+ MoO_3 system and they observed signal broadening and difference in the reduction temperature compared to $FePO_4$. The authors attributed these differences to a chemical interaction between $FePO_4$ and MoO_3 in the $FePO_4$+ MoO_3 crystals during reduction.

A single stage broad reduction behavior was observed up to 3 wt.% Mo loading (figure 3c and d), however, two stage reduction behavior was found at 5 wt.% Mo loading (figure 3e) on FeP in the temperature range of 800–950°C. The signals endorsed to the reduction of MoO_3 present on FeP. Approximately, a 6% higher hydrogen consumption was observed on 5Mo/FeP than the FeP in total, which might be due to the reduction of MoO_3 present on FeP. In addition, the increase in the MoO_3 reduction temperature for 5Mo/FeP over 3Mo/FeP was related to larger crystals

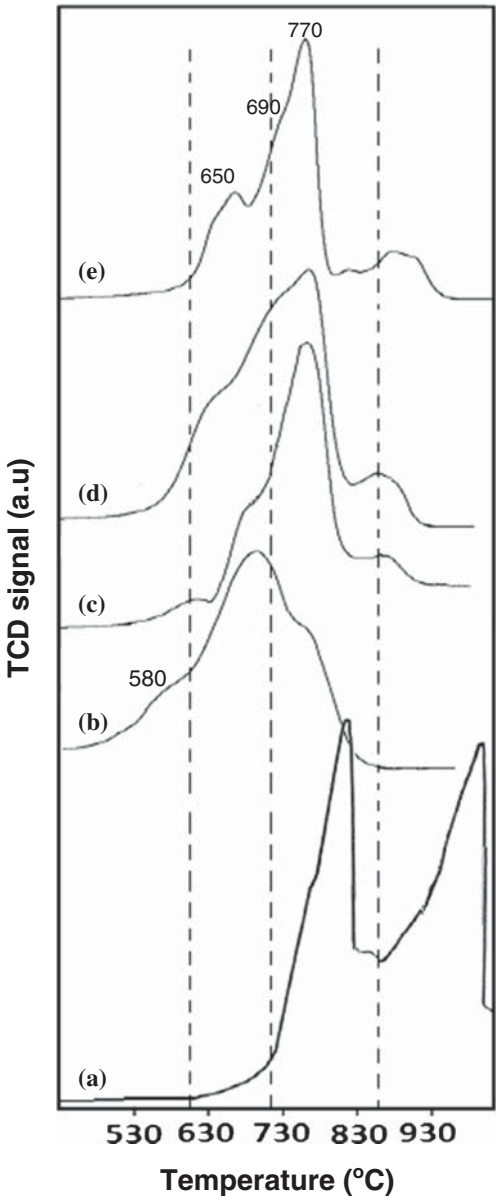

Figure 3. TPR profiles for (a) MoO_3, (b) FeP, (c) 1Mo/FeP, (d) 3Mo/FeP and (e) 5Mo/FeP Catalysts.

of MoO_3, in good agreement with XRD data (table 1). Smaller crystals are more easily reduced than the bigger ones.[5] In conclusion, addition of MoO_3 altered the reduction behavior of FeP probably due to chemical interaction under reducing conditions.

3.4 *TPD of NH_3*

Ammonia TPD results for FeP, MoO_3 and Mo/FeP catalysts are presented in figure 4 and the quantitative results are shown in table 1. Two distinct desorption peaks were observed with peak maxima at 310 and 520°C for FeP. On the other hand, MoO_3 showed a desorption peak maxima at 300°C with a shoulder

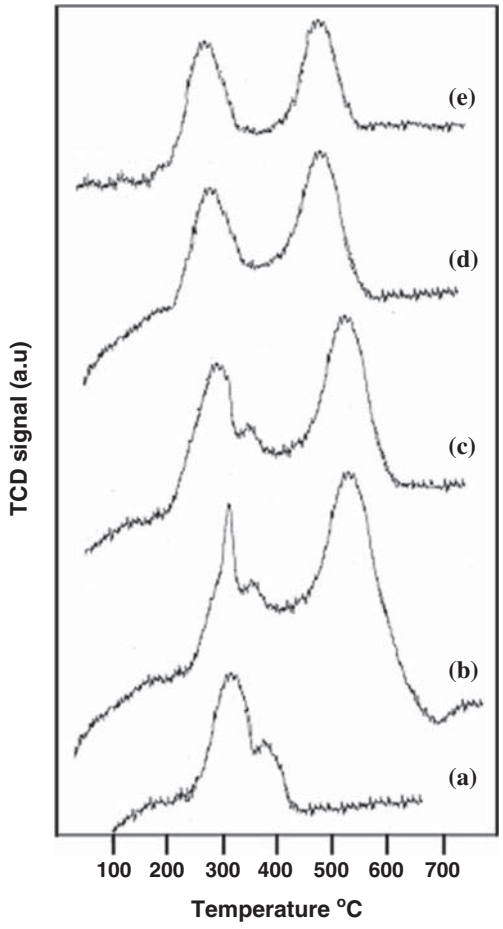

Figure 4. NH_3-TPD results for (a) MoO_3, (b) FeP, (c) 1Mo/FeP, (d) 3Mo/FeP and (e) 5Mo/FeP Catalysts.

desorption at maxima 395°C. It is well known that surface/subsurface ammonization gives low temperature desorption peaks and bulk ammonization causes a high temperature desorption.

The addition of Mo to FeP resulted in two different Mo/FeP surfaces toward NH_3 sorption. The desorption peak observed over the temperature range of 200–350°C with peak maxima around 310°C was attributed to acidic sites of medium strength. The desorption peak observed between 400 and 700°C having a peak maxima at 520°C was attributed to acidic sites of high strength. Moreover, the addition of Mo to FeP increased the moderate acid sites with proportional to Mo loading and at the same time some of the acid sites of high strength originated from FeP was reduced. The acid site strength and density was increased with increase in the surface phosphorous content in $FePO_4$.[15,16] The result revealed that some of the surface P shielding at Mo/FeP interface causing the reduction of strong acid sites originated from FeP and in agreement with HAADF/EDS data (table 1) where, the Fe and P content was decreased in proportion to Mo loading. The decreasing order of acidity was found to be as follows: FeP > 1Mo/FeP > 3Mo/FeP > 5Mo/FeP > MoO_3. Further, discussion on the influence of acidity on 2-CP selectivity will be given in Section 3.7.

3.5 *X-ray photoelectron spectroscopy*

Fe $2p_{3/2}$ binding energy (BE) in FeP and Mo/FeP was recorded at 712.0 ± 0.5 eV which indicates the presence of Fe^{3+10} species. The Mo $3d_{5/2}$ BE was recorded at 232.5 ± 0.5 eV with FWHM of 2.0 eV which suggests the existence of Mo^{6+17} in Mo/FeP catalysts. For P 2p, the binding energy recorded at 133 ± 0.5 eV indicates the presence of P^{5+} in PO_4 groups in FeP and Mo/FeP catalysts. All the catalysts displayed the O 1s BE at 530.5 ± 0.5 eV with FWHM of 1.8 eV indicating the presence of isolated oxygen in the system. The near surface Fe/Mo ratio for Mo/FeP estimated by XPS are presented in table 1. It is obvious from the result that the Fe located on the surface of the sample was depleted reasonably, while the same catalyst surface was enriched in Mo with proportional to Mo loading on Mo/FeP. It is important to mention that the maximum 2-CP yield of 68.0% was obtained on 3Mo/FeP at Fe/Mo surface ratio of 6. XPS results clearly demonstrate the MoO_3 existence on FeP.

3.6 *Influence of Mo loading and MoO_3 particle size on 2-MP ammoxidation activity*

Influence of Mo loading on the catalytic activity was studied in the ammoxidation of 2-MP to 2-CP in the temperature range of 380–420°C under atmospheric pressure. A maximum 2-MP conversion of 60% was observed on pure MoO_3, whereas, 54.0% conversion was obtained on FeP at 420°C. The high activity for MoO_3 over FeP was likely due to the presence of Mo=O on its surface which leads to complete oxidation reaction and produces high amounts of pyrazine, CO and CO_2. Figure 5a shows the Mo content in Mo/FeP played an important role on the catalytic activity. Among these catalysts, 3Mo/FeP showed about 78.0% of 2-MP conversion and only, 72.0% and 68.0% conversion was observed on 5Mo/FeP and 1Mo/FeP, respectively at 420°C. The decreasing order of activity was found to be as follows: 3Mo/FeP > 5Mo/FeP > 1Mo/FeP > MoO_3 > FeP. The study revealed that the large Mo particles observed at 5 wt.% (HAADF-EDS) was less active and on the other hand, 1 wt.% of Mo loading was inadequate to further promote the 2-MP conversion. Hence, 3 wt.% of Mo loading produced optimal composition with highly dispersed Mo particles (size 20 nm) on FeP and resulted in high activity. Based

on these outcomes, it is concluded that highly selective FeP moiety combined with certain amount of Mo=O functionality produced most active ammoxidation catalyst. Recently, Kan *et al.*[18] reported the effect of MoO_3 particle size on methane aromatization. The authors stated that nano sized MoO_3 particles were highly active and selective for aromatics over micro sized MoO_3 particles by influencing the acidity of Mo/ZSM-5.

3.7 *Influence of Mo/FeP acidity on 2-CP selectivity*

The selectivity results of 2-CP and pyrazine are presented in figure 5b. It is obvious from the results that the maximum 2-CP selectivity was observed at 400°C in all the studied catalysts. The decreasing order of 2-CP selectivity was found to be as follows: FeP (98.0%) > 1Mo/FeP (93.0%) > 3Mo/FeP (91.0%) > 5Mo/FeP (87.0%) > MoO_3(66.0%). The highest pyrazine selectivity (42.0%, 420°C) on MoO_3 was manifested due to the complete oxidation reaction. Unlike, pure MoO_3 small amount of MoO_3 present on FeP significantly reduces the undesired product pyrazine. A maximum of 21.0% pyrazine selectivity was observed at 5 wt% Mo loading on FeP at 420°C.

The relationship between acidity and 2-CP selectivity at 400°C are presented in figure 6a. TPD of NH_3 (table 1) showed the distribution of acid sites with strong and medium strength was different among the studied catalysts. The pure MoO_3 principally exhibited acid sites of moderate strength and displayed 66.0% of 2-CP selectivity. Further, FeP majorly demonstrated acid sites of high strength and showed maximum selectivity to 2-CP (∼98.0%). On the other hand, Mo/FeP catalysts displayed ample amount of both medium (Mo=O) and strong acid sites and showed slight decrease in the 2-CP selectivity compared to FeP. About 93.0% and 91.0% of 2-CP selectivity was obtained on 1Mo and 3Mo/FeP catalysts, respectively. Almost equal amount of moderate and strong acid sites on 5Mo/FeP resulted in 86.0% selectivity to 2-CP. Hence, it is possible that a catalyst composition with medium and strong acidic sites are also favorable for the ammoxidation of 2-MP to 2-CP.

Figure 6b presents the 2-CP yield results on MoO_3, FeP and Mo/FeP catalysts in the temperature range of 380–420°C. The MoO_3 showed a maximum 2-CP yield of 36.0% and on the other hand, FeP produced only 45.0% of 2-CP under similar reaction conditions (400°C, 2-MP flow rate = 2 cm^3/h). The decreased 2-CP yield for MoO_3 might be associated with complete oxidation of 2-MP (due to Mo=O groups) to undesired pyrazine, CO and CO_2 products. The 2-CP yield

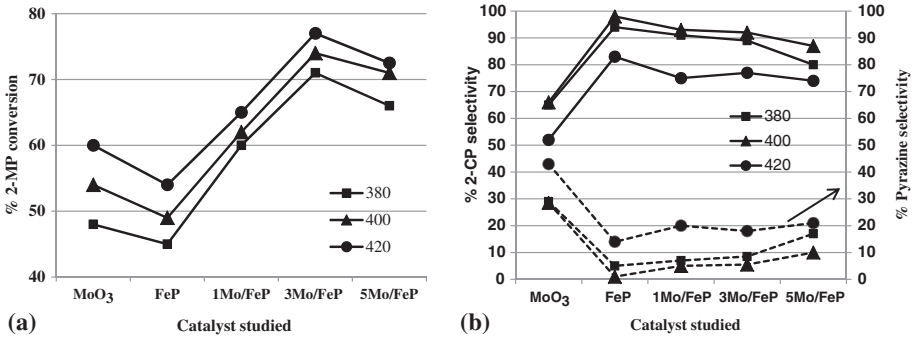

Figure 5. Results for (a) 2-MP conversion and (b) 2-CP, pyrazine selectivity. Reaction conditions. Catalyst 3g, reactant molar ratio1:13:17:38 (2MP/H_2O/NH_3/air), temperature range 380–420°C.

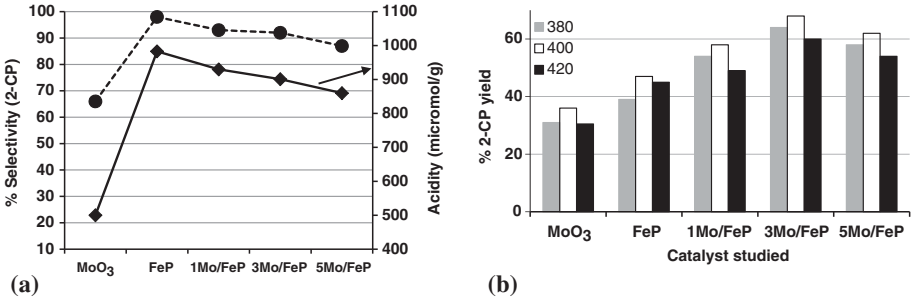

Figure 6. (a) Correlation between acidity and 2-CP selectivity at 400°C. (b) 2-CP yield results (380–420°C). Reaction conditions. Catalyst, 3g and reactant molar ratio, 1:13:17:38 (2-MP/H_2O/NH_3/air).

increased with increase in Mo loading and attained maximum yield of 68.0% on 3Mo/FeP at 400°C. Above this Mo loading, the 2-CP yield was decreased reasonably. The greater 2-CP yield on 3Mo/FeP was attributed to enhanced moderate acid sites coming from MoO_3 and cooperation between Mo and FeP at the interface in terms of oxygen and electron transfer to reactant (2-MP). Large particle formation through crystallization of MoO_3 for 5Mo/FeP could lead to the reduction of active surface and resulted in lower 2-CP yield (62.0%). In our previous report,[4] vanadium doped FeP (3V/FeP) showed a maximum 2-CP yield of 50.0% at 380°C. Recently, Martin *et al.*[19] reported a maximum 2-CP yield of 40.0% on $FeVO_4$ under similar reaction conditions. In addition, the same authors reported 2-CP yield of 50.0% on V_2O_5-Au/TiO_2.[20] The decreasing order of 2-CP yield among Mo/FeP, V/FeP and FeP was found to be as follows: 3Mo/FeP > 3V/FeP > FeP. The standard electrode redox potential of Mo^{6+} to Mo^{5+} is 0.5 V[21] and for V^{5+} to V^{4+} is 1.17 V[21] with reference to SHE (standard hydrogen electrode 0.00 V, at 1 atm and 25°C). The ease oxidation-reduction of Mo species near Mo/FeP interface was believed to be the reason for the high yields of 2-CP on Mo/FeP over V/FeP under similar reaction conditions. The reduction of Fe^{3+} to Fe^{2+} was promoted by certain action of redox between Mo^{6+} and Mo^{5+}.[8]

4. Conclusions

In the present study, the most active ammoxidation catalyst identified as 3Mo/FeP with highly dispersed Mo particles (20 nm). The average atomic composition revealed by HAADF/EDS for 3Mo/FeP as Fe 30.0%, P 40.0%, Mo 1.6% with Fe/Mo surface XPS ratio 6. The combination of enhanced moderate acidity and facile Mo/FeP interface at 3 wt% Mo loading on FeP showed greater yield of 2-CP (68%).

Acknowledgements

SABIC Chair of Catalysis, King Abudulaziz University is acknowledged for their sponsorship to this work. Special thanks to Dr. Sai Prasad, Chief Scientist, Indian Institute of Chemical technology, for his valuable suggestions to this work.

References

1. Brazdil J F and Toft M A 2010 In *Encyclopedia of Catalysis* (Wiley online library, accessed on 5 March 2015) p.3
2. Nagaraju P, Srilakshmi Ch, Pasha Nayeem, Lingaiah N, Suryanarayana I and Sai Prasad P S 2008 *Appl. Catal. A: Gen.* **334** 10
3. Nagaraju P, Srilakshmi Ch, Pasha Nayeem, Lingaiah N, Suryanarayana I and Sai Prasad P S 2008 *Catal. Today* **131** 393
4. Nagaraju P, Lingaiah N, Balaraju M and Sai Prasad P S 2008 *Appl. Catal. A: Gen.* **339** 99
5. Bhaskar T, Rajender Reddy K, Praveen Kumar Ch, Murthy M R V S and Chary K V R 2001 *Appl. Catal. A: Gen.* **211** 189
6. Teimouri A, Najari B, Chermahini A N, Salavati H and Fazel-Najafabadi M 2014 *RSC. Adv.* **4** 37679
7. Ai M 2002 *Appl. Catal. A: Gen.* **232** 1
8. Ai M 2002 *Appl. Catal. A: Gen.* **234** 235
9. Ai M and Ohdan K 1997 *Appl. Catal. A: Gen.* **165** 461
10. Wang X, Wang Y, Tang Q, Guo Q, Zhang Q and Wan H 2003 *J. Catal.* **21** 7457
11. Al-Anazi F F N 2006 In *Propane oxidative dehydrogenation to propene using molybdenum phosphate catalysts* (Ph.D thesis: Cardiff University UK) p.77 and p.85
12. Mehri S, Reine W, Andersson A, Susan J and Yanping T 1991 *J. Catal.* **132** 128
13. Thomas R, de Beer V H J and Moulijn J A 1981 *Bull. Chim. Belg.* **12** 90
14. Rensel D J, Rouvimov S, Gin M E and Hicks J C 2013 *J. Catal.* **305** 256
15. Wendt G and Lindstrom C F 1976 *Z. Chem.* **12** 500
16. Chen Y-W, Wang P-J and Wang W-J 1990 *Catal. Lett.* **6** 187
17. Poulston S, Price N J, Weeks C, Allen M D, Parlett P, Steinberg M and Bowker M 1998 *J. Catal.* **178** 658
18. Hu J, Wu S, Ma Y, Yang X, Li Z, Liu H, Huo Q, Guan J and Kan Q 2015 *New J. Chem.* **39** 5459
19. Naresh D, Venkata Narayana K, Brückner A and Martin A 2012 *Appl. Catal. A: Gen.* **443–444** 111
20. Alshammari A, Kalevaru V N, Dhachapally N, Kockritz A, Bagabas A and Martin A 2015 *Top. Catal.* **58** 1062
21. Bratsch G S 1989 *J. Phys. Chem. Ref. Data* **18** 7